

Insilico Studies on Bioactive Compounds from *Solanum Nigrum* as Phospholipase A2 Inhibitors

Veerapandi Loganathan, Lekhashri Vijayan, Riya Mariyam Rinu, Ahalya Madhu



Abstract: The prevalence of high mortality rates due to snake bites is widely found in Indian farmlands, as most poisonous snake varieties are found in these areas. Although many antivenoms, like antivenin, have been formulated to treat snake bites, they have limitations, such as high cost and difficulties in storage. Most deaths are primarily due to the time delay in treating snakebites. The venom's activity, or its poisonous nature, has been attributed to enzymes such as Phospholipase A2, hyaluronidase, and protease. As a solution for this problem, the active site of these enzymes can be elucidated and inhibited using extracts from plants and food sources through docking studies. Literature reports suggest that *Solanum nigrum* compounds have shown high inhibitory activity. In this study, we analysed a list of upregulated compounds in response to venom enzymes. From the analysis, we filtered out eight possible compounds. A docking study was carried out on these bioactive compounds in *Solanum nigrum*. The mode of interaction of the bioactive compound was studied using AutoDock software. Insilico molecular docking and molecular dynamics simulation were performed using Phospholipase A2 (1BK9) to understand the conformational changes and to analyse the optimal binding pocket. Analysis shows that it has very favourable predicted binding energy. The bonding interaction was formed between the active site of PLA2 and bioactive compounds. From the results, it has been observed that beta-sitosterol exhibits a favourable interaction with PLA2 (1BK9) compared to other bioactive compounds.

Keywords: Snake bite; Antivenom; *Solanum nigrum*; Molecular docking; Molecular Dynamics; PLA2.

I. INTRODUCTION

In India, morbidity and mortality rates are excessive. Annually, 50000 people die due to snake bites. It is a most unnoticed issue in many rural and urban states. Treatment for snake bites is a serious medical issue, especially in rural areas where snakes are abundant. *Daboia russelli*, *Echis carinatus*, *Naja kaouthia*, and *Naja Naja* are the most common snakes found in Tamil Nadu, and a vast number of deaths occur due to inadequate knowledge about snake bites and improper treatment against snake bites.

Manuscript received on 25 February 2023 | Revised Manuscript received on 28 March 2023 | Manuscript Accepted on 15 June 2023 | Manuscript published on 30 June 2023.

*Correspondence Author(s)

Veerapandi Loganathan*, Assistant Professor, Department of Food Technology, Nehru Institute of Technology, Kaliyapuram, Coimbatore (Tamil Nadu), India. Email ID: veerapandiloganathan@gmail.com

Lekhashri Vijayan, Department of Food Technology, Saintgits College of Engineering, Kottukulam, Pathamuttom Hills, Kottayam (Kerala), India. Email ID: lekhamukund115@gmail.com

Riya Mariyam Rinu, Department of Food Technology, Saintgits College of Engineering, Kottukulam, Pathamuttom Hills, Kottayam (Kerala), India. Email ID: riyarittu85@gmail.com

Ahalya Madhu, Department of Food Technology, Saintgits College of Engineering, Kottukulam, Pathamuttom Hills, Kottayam (Kerala), India. Email ID: Ahalyamadhu2001@gmail.com

© The Authors. Published by Lattice Science Publication (LSP). This is an open access article under the CC-BY-NC-ND license (<http://creativecommons.org/licenses/by-nc-nd/4.0/>)

Snake venoms are primarily characterised as neurotoxic and hemotoxic. Snake venom contains a high amount of phospholipase A (PLA) enzymes, which can induce several pharmacological effects, such as pre- and post-neurotoxicity, hemolysis, anti-coagulation, platelet aggregation, and cardiotoxicity. PLA enzymes catalyse the hydrolysis of the 2-acyl ester bond of 3-sn-phospholipids, producing fatty acids such as arachidonic acid (an unsaturated fatty acid) and lysophospholipids. Arachidonic acid acts as an inflammatory precursor, leading to the formation of eicosanoids. The only treatment for snakebite is antiserum, but its low efficacy is due to several reasons, and it also presents several difficulties, including marketing, storage, and economic concerns. Several medicinal plant sources are used in traditional treatments against various snakebites. Plant bioactive compounds have been able to inhibit the activity of snake venom enzymes, and those compounds may be helpful for the development of anti-snake venom drugs against snake bites in the future. *Solanum nigrum* fruits are suggested in Ayurveda for treating snake-bitten patients. A phytochemical study on *Solanum nigrum* reported several compounds, which are present in higher concentrations in the fruits of *Solanum nigrum*.

Black nightshade (*Solanum nigrum*), commonly known as Makoi in India, has been traditionally used in Southeast Asia, particularly the Indian subcontinent, as a panacea for several ailments (especially liver disorders) since time immemorial (Li et al., 2009; Nawab et al., 2012 [26]; Wannang et al., 2008 [33]; Lee & Lim, 2003 [15]; Javed et al., 2011 [11]; Kang, Jeong & Choi, 2011 [13]; Lin et al., 2008 [21]; Hsieh, Fang & Lina, 2008 [7]). *Solanum* sp. have been reported to possess a broad spectrum of activities viz. cytotoxic (Mahadevi et al., 2015 [23]), antifungal (Singh et al., 2007 [31]), antiviral (Arthan et al., 2002 [4]), molluscicidal (Silva et al., 2006 [30]), antimalarial (Makinde, Obih & Jimoh, 1987 [24]), etc. Extracts of various plant parts of the genus have been shown to possess potent anticancer (Patel et al., 2009 [20] [28]; Raju et al., 2003 [29]), antimicrobial (Al-Fatimi et al., 2007 [3]) and antiulcerogenic activities (Jainu & Devi, 2006 [10]). Recently, considerable attention has been directed towards the anticancer potential of the herb *S. nigrum*. However, the mechanism(s) underlying the growth inhibitory and apoptosis-inducing activity of *S. nigrum* have still not been adequately understood or elucidated (Gabrani et al., 2012 [6]). *S. nigrum* is rich in SGAs (Agarwal et al., 2010 [1]; Jain et al., 2011 [9]) viz. solasodine, solanidine, alpha-solanine, solasonine, solamargine, diosgenin, solavilline and solasdamine (Kuo et al., 2000 [14]; Liu et al., 2004 [22]; Chang et al., 1998 [5]; Huang, Syu & Jen-kun Lin, 2010 [8]), most of which have been reported to possess possible antitumor properties though

they have not been thoroughly investigated (Li et al., 2008b [19]). The cytotoxic activity of both crude extracts and isolated components has been evaluated against a panel of cancer cell lines, viz. HepG2 (Ji et al., 2008 [12]), HT29 (Lee et al., 2004a [16]), HCT-116 (Lee et al., 2004b [17]), MCF-7 (Son et al., 2003 [32]), U14 (Li et al., 2008a [18]), HeLa (Oh & Lim, 2007 [27]) as well as standard cell lines (Moglad et al., 2014 [25]) and on animal models of cancer.

However, human and drug resources would certainly be wasted while the molecule is being cleared for use in clinical studies. In this regard, computational techniques are used to forecast the pharmacokinetic characteristics of humans. With various degrees of complexity for the compound screening of massive data sets, many in silico ADME (absorption, distribution, metabolism, excretion) models have been developed. Modern in silico techniques outperform traditional investigative procedures in terms of speed, ease of use, and cost. Due to the toxicity or latency of ideal conditions at the moment, pharmacokinetic characteristics are high rates of preclinical testing in pharmaceutical companies and the clinical industry. Medical chemists may be able to manage a molecule's pharmacokinetic and toxicological characteristics through alterations to the structure.

II. MATERIALS AND METHODS

A. Selection of Sample

Fruits were collected from the Western Ghats Forest range. The fruits were washed under running tap water, crushed with a little amount of water, and the extracted samples were labelled, and the percentage of the sample was recorded.

B. Accession of 3D Structure of Target Protein

The 3D structure of a different protein with a 124-sequence length and three unique ligands was obtained from the Protein Data Bank online server.

C. Preparation of Target Protein

The newly modelled protein structure was protonated using the AutoDock tools program, and thereafter, the obtained structure was energy-minimised and saved in PDBQT format.

D. Preparation of Ligands

The structures of phenolic lead molecules (L1 to L7) were drawn and energy-minimised using Schrodinger Maestro software and saved in PDB format. For each compound, the most stable conformation was used in the docking calculation, and the AutoDock tools program was employed to generate the docking input files in PDBQT format.

E. Binding Pocket

The protein structure was uploaded to the online server DoG-SiteScorer in PDB format to assess the most suitable binding pocket based on druggability. The three-dimensional parameters of the most druggable binding pockets were used to dock lead compounds with the target proteins.

F. Docking Studies

The PDB formats of all experimental phenolic derivatives were prepared and quality-checked to form a PDBQT file using AutoDock tools.

All the lead molecules (L1 – L7) were docked separately against 1BK9 using AutoDock software. The predicted

docked complexes were evaluated based on the lowest binding energy (kcal/mol) values, and three-dimensional graphical depictions of all the docked complexes were generated using Schrodinger Maestro. The best docked molecules were subjected to molecular dynamics (MD) simulation.

G. Molecular Dynamics (MD) Simulations

The best docked energy (Kcal/mol) complexes (L1) were selected for MD simulations study. This study was performed using the Groningen Machine for Chemical Simulations (GROMACS) 4.5.4 package with the GROMOS 53A6 force field and the SPC216 water model. The topology files for the receptor and ligand were created using the GROMOS 53A6 force field and the online PRODRG Server. The receptor–ligand complexes were then placed in the middle of a cubic box with 0.9 Å distance. The energy minimisation (n steps = 50,000) was performed using a steepest descent approach (1000 ps), and the energy calculation was carried out using the particle mesh Ewald (PME) method.

III. RESULTS AND DISCUSSION

Isolation of compounds from the extract of *S. nigrum* fruits. *Solanum nigrum* fruits were selected based on the phytochemical separations. The isolated compounds are betasitosterol (L1), (Z, E)-4, 6, 8-megastigmatriene, pinosresinol, medioresinol, phytol, dillapiole, and scopoletin.

A. Chemoinformatic

All amino acid lead derivatives complied with rule of five, with excellent aqueous solubility and good oral bioavailability. Table 1 refers to the chemoinformatic properties of amino acid derivatives, which clearly show that all phenolic derivatives from L1 to L7 possess good and acceptable physicochemical properties like molecular weight, flexibility, hydrogen bond donor, hydrogen bond acceptor, solubility and no violation of Lipinski rule. The active site of the PLA2 complex (*Naja naja*), used for docking studies, was identified using the RCSB protein data bank server. The aqueous extract of *Solanum nigrum* fruits contained several phytochemicals, as determined in a study, including betasitosterol, (Z, E)-4, 6, 8-megastigmatriene, pinosresinol, medioresinol, phytol, tetracosanoic acid, dillapiole, and scopoletin, which were expected to exhibit *Naja naja* enzyme inhibition activity. These selected compounds are bound to the active site residues of PLA₂. The crystal structure of the PLA2 complex, covalently modified by p-bromophenacyl-bromide (pBPB), was determined to a resolution of 2.0 Å and refined to a crystallographic R factor of 15.3%. The p-bromophenacyl group near the active site occupies a position similar to that in pBPB modified PLA2. The binding of pBPB to APLA2 induces no other significant conformational changes in the enzyme molecule.

The graph shown in Figure reveals that most of the derivatives show one violation of each rule, and few structures, viz. L1, L2, L3, L4, L5, L6 and L7 did not show any violation. Hence, they can be provisionally approved for preclinical trials. The structures that show three breaches of the Muegge and

Ghose filters must be excluded from further preclinical processes. In Tables 1 & 2, it is clear that the structures did not show any violation, and most of the derivatives violate more than one rule for each filter. Only four compounds fall within the allowed range of physicochemical properties and satisfy all the key parameters.

B. Molecular Docking Analysis

To identify the compound at the binding site of the target protein by docking. In this tool, ChemSketch is used for drawing structures and ligand preparations. Autodock 4 programs acknowledge docking. The target protein is prepared by adding atomic solvation parameters, Kollman charges, and polar hydrogen bonds. On Cygwin, auto-dock computations and auto-grid were performed. Using UCSF chimera, hydrogen bonding and hydrophobic interactions between docked ligands and macromolecule targets were analysed.

The active site of PLA2 complex 1BK9 (*Naja naja*), as shown in Table 3, which was used for the docking study, was identified using the RCSB protein data bank server. The aqueous extract of *Solanum nigrum* fruits contains several phytochemicals. We have selected the major compounds betasitosterol, (Z, E)-4, 6, 8-megastigmatriene, pinosresinol, medioresinol, phytol, dillapiole, and scopoletin, which are expected to exhibit *Naja naja* enzyme inhibition activity. These selected compounds interact with the active site residues of PLA₂. The crystal structure of the PLA2 complex, with a 124-amino acid sequence and covalently modified by p-bromophenacyl-bromide (pBPB), was determined to a resolution of 2.0 Å and refined to a crystallographic R factor of 15.3%. The p-bromo-phenacyl group near the active site occupies a position similar to that in pBPB modified PLA2. The binding of PLA2 induces no other significant conformational changes in the enzyme molecule. The crystal structure of the PLA2 complex, covalently modified by p-bromo-phenacyl-bromide, was determined to a resolution of 2.0 Å and refined to a crystallographic R factor of 15.3%. The p-bromo-phenacyl group near the active site occupies a position similar to that in pBPB modified PLA2. The binding of pBPB to APLA2 induces no other significant conformational changes in the enzyme molecule. The p-bromo-phenacyl-bromide covalently bound to the NDI atom of His48 fits well in the hydrophobic channel, forming extensive hydrophobic interactions with the surrounding residues, especially with the side chains of Phe5 and Cys45 and the main chain of Gly30. Some pharmacological effects, as well as the catalytic and disintegrin activities, were abolished by p-bromophenacyl bromide, which covalently binds to residue His48 in the catalytic site. Additionally, the anticoagulant activity has also been abolished by p-bromophenacyl-bromide. This prompted us to dock 1BK9 with p-bromophenacyl-bromide. Upon docking, p-bromophenacyl-bromide interacts with the 1BK9 complex, with a binding energy of -5.15 kcal/mol, as mentioned in Table 4. It interacts with the following residues: Phe5, His48, Cys29, Gly31, and Asp49. Analysis shows that it has very favourable predicted binding energy.

Phytosterols are widely found in plants, animals, and fungi, and share a structural similarity with cholesterol. This prompted us to dock 1BK9 with beta sitosterol. Upon

docking, beta-sitosterol interacts with the 1BK9 complex, exhibiting a binding energy of -10.25 kcal/mol. It interacts with the following residues: ILE9, PHE5, HIS48, PHE106, CYS45, TRP31, TYR52, and LEU2. The best ligand pose was selected based on the lowest binding energy confirmation. Upon docking studies with respect of various molecules, Dillapiole interacts with the 1BK9 with binding energy of -6.52kcal/mol, medioresinol (-3.72kcal/mol), (Z, E)-4, 6, 8-megastigmatriene (-6.52kcal/mol), pinosresinol (-5.50kcal/mol), Phytol (-5.82kcal/mol), scopoletin (-3.83kcal/mol), tetracosonicacid (-2.01kcal/mol). From the docking studies, it is observed that the binding energy of the PLA2 (1BK9) – beta sitosterol complex can be considered a potent inhibitor of 1BK9 when compared with all other complexes.

The crystal structure of the PLA2 complex, covalently modified by p-bromo-phenacyl-bromide, was determined to a resolution of 2.0 Å and refined to a crystallographic R factor of 15.3%. The p-bromo-phenacyl group near the active site occupies a position similar to that in pBPB modified PLA2. The binding of pBPB to APLA2 induces no other significant conformational changes in the enzyme molecule. The p-bromo-phenacyl-bromide covalently bound to the NDI atom of His48 fits well in the hydrophobic channel, forming extensive hydrophobic interactions with the surrounding residues, especially with the side chains of Phe5 and Cys45 and the main chain of Gly30. Some pharmacological effects, as well as the catalytic and disintegrating activities, were abolished by p-bromophenacyl bromide, which covalently binds to residue His48 in the catalytic site. Additionally, the anticoagulant activity has also been abolished by p-bromophenacyl-bromide. This prompted us to dock 1BK9 with p-bromophenacyl-bromide. Upon docking, p-bromophenacyl-bromide interacts with the 1BK9 complex with binding energy of -5.15kcal/mol. It interacts with the following residues: Phe5, His48, Cys29, Gly31, and Asp49. Analysis shows that it has very favourable predicted binding energy.

Phytosterols are widely found in plants, animals, and fungi, and share a structural similarity with cholesterol. This prompted us to dock 1BK9 with beta sitosterol. Upon docking, beta-sitosterol interacts with the 1BK9 complex, exhibiting a binding energy of -10.51 kcal/mol. It interacts with the following residues: ILE104, CYS44, ARG43, ASN109, VAL47, CYS105, and ALA101. The best ligand pose was selected based on the lowest binding energy confirmation. Upon docking studies with respect of various molecules, Dillapiole interacts with the 1BK9 with binding energy of -5.77kcal/mol, medioresinol (-7.09kcal/mol), (Z, E)-4, 6, 8-megastigmatriene (-6.81kcal/mol), pinosresinol (-8.45kcal/mol), Phytol (-6.78kcal/mol), scopoletin (-5.82kcal/mol). From the docking studies, it is observed that the binding energy of the PLA2 (1BK9) – beta sitosterol complex can be considered a potent inhibitor of 1BK9 when compared with all other complexes.

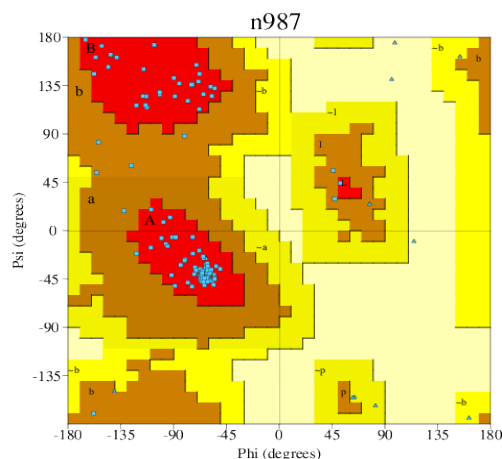


[Fig.2: Ramachandran plot of 1BK9]

C. Molecular Dynamics

A molecular dynamics simulation of the Phospholipase A2 (1bk9)–beta sitosterol complex was performed using the GROMACS software to assess the stability of the complex. The simulation was carried out till 20 nanoseconds. It is observed from the RMSD graph that the protein becomes stabilised around eight nanoseconds, with an average variation of 0.25 nm to 0.35 nm. The RMSF graph (Figure 4) shows that the protein is almost rigid, with a range of 0.05 nm to 0.2 nm, except for specific residues. The gyration graph 5 shows that there were not many changes in the compactness of the protein throughout the simulation.

Throughout the complex simulation, the PDB structure of the 1BK9-Betasitosterol Complex is retrieved at certain intervals and analysed for binding residues. Specific Residues are found to bind with beta-sitosterol at all conformational changes. After the protein has been stabilized, the following binding residues are ILE104, CYS44, ARG43, ASN109, VAL47, CYS105, and ALA101. The three-dimensional crystal structure of IBK9 enzyme was successfully built using the online I-Tasser server. It was validated by constructing a Ramachandran plot (Figure 2), which revealed that 96% of the residues fell within the favourable quadrant of the plot. The snapshots of the structures obtained at regular intervals during the simulation showed that there were few secondary structural variations at specific time frames. To further confirm the secondary structural changes, we tracked the secondary structural changes throughout the simulation and found that residues 79 to 83, which are part of a beta-strand at the beginning, turned into a loop around 15 ns. Similarly, residue 116, which formed a small helix, was deformed entirely into a loop after 10ns.

IV. DISCUSSION

The Insilico docking was performed to study the interaction between *p*-bromophenacyl bromide and those compounds with Phospholipase A2 (1BK9). From the results, it is observed that the binding energy of *p*-Bromo phenacyl bromide - 1BK9 complex has -10.51, 1BK9 - Dillapiole and 1BK9 - scopoletin complex is almost equal it has -5.77 and -5.82 respectively, 1BK9 – (Z, E)-4, 6, 8-megastigmatriene and 1BK9 - phytol complex is almost equal it has -6.81 and -6.78, 1BK9 – pinoresinol, 1BK9 - mediresinol complex have

second and third highest binding energy it has -8.45, and -7.09. The beta-sitosterol and 1BK9 complex has a higher binding energy compared to other compounds, as well as the 1BK9–BPBP complex. Thus, beta sitosterol is more likely to bind to 1BK9 rather than BPBP. This could be a possible reason for making a drug. Molecular Dynamics Simulation of the Phospholipase A2 (1BK9)–Beta sitosterol complex was performed to assess the stability of the complex. The simulation was carried out for 20 nanoseconds, as shown in Figures 6 & 7. It is observed from the results that the protein gets stabilised initially, from 0 to 4 nanoseconds. After four nanoseconds, it deviates slightly and then becomes fully stabilised. Throughout the complex simulation, specific residues are found to bind with beta-sitosterol at all conformational changes.

V. CONCLUSION

In conclusion, we hypothesise that beta-sitosterol has the affinity to bind with PLA2 (1BK9) competitively. This could be a possible reason for making a drug. *Solanum nigrum* proteins might function as co-neutralizing agents and might reduce the toxicity of venomous snakes such as *Naja naja*, the venom of which shares high sequence homology with the venom of *Naja naja*, whose natural habitat is in the Arabian Peninsula.

The primary conclusion of this study is that *Solanum nigrum* proteins have potential use as co-neutralising agents to mitigate the toxicity of certain venomous snakes, such as *Naja naja*. The potency of antivenom antibodies can be increased with the use of highly concentrated plant protein extracts.

DECLARATION STATEMENT

After aggregating input from all authors, I must verify the accuracy of the following information as the article's author.

- **Conflicts of Interest/ Competing Interests:** Based on my understanding, this article has no conflicts of interest.
- **Funding Support:** This article has not been funded by any organizations or agencies. This independence ensures that the research is conducted with objectivity and without any external influence.
- **Ethical Approval and Consent to Participate:** The content of this article does not necessitate ethical approval or consent to participate with supporting documentation.
- **Data Access Statement and Material Availability:** The adequate resources of this article are publicly accessible.
- **Author's Contributions:** The authorship of this article is contributed equally to all participating individuals.

REFERENCES

1. Agarwal et al. (2010). Agarwal AD, Bajpei PS, Patil A, Sunil R. *Solanum torvum*—a phytopharmacological review. *Scholars Research Library*. 2010;2:403–

2. 407. <https://www.scholarsresearchlibrary.com/articles/solanum-torvum-sw--a-phytopharmacological-review.pdf>
3. Al-Fatimi et al. (2007) Al-Fatimi M, Wurster M, Schroder G, Lindequist U. Antioxidant, antimicrobial and cytotoxic activities of selected medicinal plants from Yemen. *Journal of Ethnopharmacology*. 2007;111:657–666. <http://doi.org/10.1016/j.jep.2007.01.018>
4. Arthan et al. (2002). Arthan D, Svasti J, Kittakooop P, Pittayakhachonwut D, Tanticharoen M, Thebtaranonth Y. Antiviral iso-flavonoid sulfate and steroidal glycosides from the fruits of *Solanum torvum*. *Phytochemistry*. 2002;59:459–463. [http://doi.org/10.1016/S0031-9422\(01\)00417-4](http://doi.org/10.1016/S0031-9422(01)00417-4)
5. Chang et al. (1998) Chang LC, Tsai TR, Wang JJ, Lin CN, Kuo KW. The rhamnose moiety of solamargine plays a crucial role in triggering cell death by apoptosis. *Biochemical and Biophysical Research Communications*. 1998;242:21–25. <https://doi.org/10.1006/bbrc.1997.7903>
6. Gabrani et al. (2012). Gabrani R, Jain R, Sharma A, Sarethy IP, Dang S, Gupta S. Antiproliferative effect of *Solanum nigrum* on human leukemic cell lines. *Indian Journal of Pharmaceutical Sciences*. 2012;74:451–453. <http://doi.org/10.4103/0250-474X.108421>
7. Hsieh, Fang & Lina (2008) Hsieh CC, Fang HL, Lina WC. Inhibitory effect of *Solanum nigrum* on thioacetamide-induced liver fibrosis in mice. *Journal of Ethnopharmacology*. 2008;119:117–121. <http://doi.org/10.1016/j.jep.2008.06.002>
8. Huang, Syu & Jen-kun Lin (2010) Huang HC, Syu K, Jen-kun Lin JK. Chemical Composition of *Solanum nigrum* Linn. extract and induction of autophagy by leaf water extract and its major flavonoids in AU565 breast cancer cells. *Journal of Agricultural and Food Chemistry*. 2010;58:8699–8708. <http://doi.org/10.1021/jf101003v>
9. Jain et al. (2011) Jain R, Sharma A, Gupta S, Sarethy IP, Gabrani R. *Solanum nigrum*: current perspectives on therapeutic properties. *Alternative Medicine Review*. 2011;16:78–85. <https://pubmed.ncbi.nlm.nih.gov/21438649/>
10. Jainu & Devi (2006). Jainu M, Devi CS. Antulcerogenic and ulcer healing effects of *Solanum nigrum* on experimental ulcer models: possible mechanism for the inhibition of acid formation. *Journal of Ethnopharmacology*. 2006;104:156–163. <http://doi.org/10.1016/j.jep.2005.08.064>
11. Javed et al. (2011) Javed T, Ashfaq UA, Riaz S, Rehman S, Riazuddin S. In vitro antiviral activity of *Solanum nigrum* against hepatitis C virus. *Virology Journal*. 2011;8:26–32. <http://doi.org/10.1186/1743-422X-8-26>
12. Ji et al. (2008) Ji YB, Gao SY, Ji CF, Zou X. Induction of apoptosis in HepG2 cells by solanine and Bcl-2 protein. *Journal of Ethnopharmacology*. 2008;115:194–202. <http://doi.org/10.1016/j.jep.2007.09.023>
13. Kang, Jeong & Choi (2011) Kang H, Jeong HD, Choi HY. The chloroform fraction of *Solanum nigrum* suppresses nitric oxide and tumour necrosis factor- α in LPS-stimulated mouse peritoneal macrophages through inhibition of p38, JNK and ERK1/2. *American Journal of Chinese Medicine*. 2011;39:1261–1273. <http://doi.org/10.1142/S0192415X11009548>
14. Kuo et al. (2000) Kuo KW, Hsu SH, Li YP, Lin WL, Liu LF, Chang LC, Lin CC, Lin CN, Sheu HM. Anticancer activity evaluation of the *Solanum glycoalkaloid* solamargine. Triggering apoptosis in human hepatoma cells. *Biochemical Pharmacology*. 2000;60:1865–1873. [http://doi.org/10.1016/S0006-2952\(00\)00506-2](http://doi.org/10.1016/S0006-2952(00)00506-2)
15. Lee & Lim (2003) Lee SJ, Lim KT. Antioxidative effects of glycoprotein isolated from *Solanum nigrum* Linn. on oxygen radicals and its cytotoxic effects on the MCF-7 cell. *Journal of Food Science*. 2003;68:466–470. <http://doi.org/10.1111/j.1365-2621.2003.tb05695.x>
16. Lee et al. (2004a) Lee KR, Kozukue N, Han JS, Park JH, Chang EY, Baek EJ, Chang JS, Friedman M. Glycoalkaloids and metabolites inhibit the growth of human colon (HT29) and liver (HepG2) cancer cells. *Journal of Agricultural and Food Chemistry*. 2004a;52:2832–2839. <http://doi.org/10.1021/jf030526d>
17. Lee et al. (2004b) Lee SJ, Oh PS, Ko JH, Lim K, Lim KT. A 150-kDa glycoprotein isolated from *Solanum nigrum* L. has cytotoxic and apoptotic effects by inhibiting the effects of protein kinase C alpha, nuclear factor-kappa B and inducible nitric oxide in HCT-116 cells. *Cancer Chemotherapy and Pharmacology*. 2004b;54:562–572. <http://doi.org/10.1007/s00280-004-0850-x>
18. Li et al. (2008a) Li J, Li Q, Feng T, Li K. Aqueous extract of *Solanum nigrum* inhibit growth of cervical carcinoma (U14) via modulating immune response of tumour-bearing mice and inducing apoptosis of tumour cells. *Fitoterap*. 2008a;79:548–556. <http://doi.org/10.1016/j.fitote.2008.06.010>
19. Li et al. (2008b) Li J, Li QW, Gao DW, Han ZS, Li K. Antitumor effects of total alkaloids isolated from *Solanum nigrum* in vitro and in vivo. *Pharmazie*. 2008b;63:534–538. <https://pubmed.ncbi.nlm.nih.gov/18717490/>
20. Li et al. (2009) Li J, Li QW, Gao DW, Han ZS, Lu WZ. Antitumor and immunomodulating effects of polysaccharides isolated from *Solanum nigrum* Linn. *Phytotherapy Research*. 2009;23:1524–1530. <https://doi.org/10.1002/ptr.2769>
21. Lin et al. (2008) Lin HM, Tseng HC, Wang CJ, Lin JJ, Lo CW, Chou FP. Hepatoprotective effects of *Solanum nigrum* Linn. extract against CCl4-induced oxidative damage in rats. *Chemico-Biological Interactions*. 2008;171:283–293. <http://doi.org/10.1016/j.cbi.2007.08.008>
22. Liu et al. (2004) Liu LF, Liang CH, Shiu LY, Lin WL, Lin CC, Kuo KW. Action of solamargine on human lung cancer cells—enhancement of the susceptibility of cancer cells to TNFs. *FEBS Letters*. 2004;577:67–74. <http://doi.org/10.1016/j.febslet.2004.09.064>
23. Mahadevi et al. (2015) Mahadevi R, Ramakrishnaiah H, Krishna V, Deepalakshmi AP, Kumar NN. Cytotoxic activity of methanolic extracts of *Solanum erianthum* D. Don. *International Journal of Pharmacy and Pharmaceutical Sciences*. 2015;7:106–108. https://www.researchgate.net/publication/308019113_Cytotoxic_activity_of_methanolic_extract_of_Solanum_rianthum_D_Don
24. Makinde, Obih & Jimoh (1987) Makinde JM, Obih PO, Jimoh AA. Effect of *Solanum erianthum* aqueous leaf extract on *Plasmodium berghei* in mice. *African Journal of Medicine and Medical Sciences*. 1987;16:193–196. <https://pubmed.ncbi.nlm.nih.gov/2830780/>
25. Moglad et al. (2014) Moglad EHO, Abdalla OM, Koko WS, Saadabi AM. In vitro anticancer activity and cytotoxicity of *Solanum nigrum* on cancers and regular cell lines. *International Journal of Cancer Research*. 2014;10:74–80. <http://doi.org/10.3923/ijcr.2014.74.80>
26. Nawab et al. (2012). Nawab A, Thakur VS, Yunus M, Ali Mahdi A, Gupta S. Selective cell cycle arrest and induction of apoptosis in human prostate cancer cells by a polyphenol-rich extract of *Solanum nigrum*. *International Journal of Molecular Medicine*. 2012;29:277–284. <http://doi.org/10.3892/ijmm.2011.835>
27. Oh & Lim (2007). Oh, P.S., Lim KT. HeLa cells treated with phytylglycoprotein (150 kDa) were killed by activation of caspase three via inhibitory activities of NF-kappaB and AP-1. *Journal of Biomedical Science*. 2007;14:223–232. <http://doi.org/10.1007/s11373-006-9140-4>
28. Patel et al. (2009) Patel S, Gheewala N, Suthar A, Shah A. In-vitro cytotoxicity activity of *Solanum nigrum* extract against HeLa cell line and Vero cell line. *International Journal of Pharmacy and Pharmaceutical Sciences*. 2009;1:38–46. https://www.researchgate.net/publication/228492173_In-Vitro_cytotoxicity_activity_of_Solanum_Nigrum_extract_against_Hela_cell_line_and_Vero_cell_line
29. Raju et al. (2003) Raju K, Anbuganapathi G, Gokulakrishnan V, Rajkaoppr B, Jayakar B, Manian S. Effect of dried fruits of *Solanum Nigrum* against CCl4-induced hepatic damage in rats. *Biological and Pharmaceutical Bulletin*. 2003;26:1618–1629. <http://doi.org/10.1248/bpb.26.1618>
30. Silva et al. (2006) Silva T, Camara C, Agra F, Carvalho M, Frana M, Brandoline S, Da Silva Paschoal L, Braz-Filho R. Molluscicidal activity of *Solanum* species of the northeast of Brazil on *Biomphalaria glabrata*. *Fitoterap*. 2006;77:449–452. <http://doi.org/10.1016/j.fitote.2006.05.007>
31. Singh et al. (2007) Singh O, Subharani K, Singh N, Devi N, Nevidita L. Isolation of steroidal glycosides from *Solanum xanthocarpum* and studies on their antifungal activities. *Natural Product Research*. 2007;21:585–590. <http://doi.org/10.1080/14786410701369458>
32. Son et al. (2003) Son YO, Kim J, Lim JC, Chung Y, Chung GH, Lee JC. Ripe fruit of *Solanum nigrum* L. inhibits cell growth and induces apoptosis in MCF-7 cells. *Food and Chemical Toxicology*. 2003;41:1421–1428. [http://doi.org/10.1016/S0278-6915\(03\)00161-3](http://doi.org/10.1016/S0278-6915(03)00161-3)
33. Wannang et al. (2008) Wannang NN, Anuka JA, Kwanashie HO, Gyang SS, Auta A. Antiseizure activity of the aqueous leaf extract of *Solanum nigrum* Linn (Solanaceae) in experimental animals. *African Health Sciences*. 2008;8:74–79. <https://pubmed.ncbi.nlm.nih.gov/19357754/>



SUPPLEMENTARY DATA

Table I: Chemoinformatic Properties of Selected Compounds

Physicochemical properties	L1	L2	L3	L4	L5	L6	L7
Molecular weight (g/mol)	414.91	176.30	358.39	388.41	296.53	222.24	192.17
Log P	4.79	3.15	2.67	3.29	4.71	2.82	1.86
Log S	-7.90	-3.38	-3.58	-3.65	-5.98	-2.96	-2.46
H-Bond acceptor	1	0	6	7	1	4	4
H- Bond Donor	1	0	2	2	1	0	1
Molar refractivity	133.23	60.81	94.90	101.39	98.94	59.59	51.00
Heavy atoms	30	13	26	12	0	16	14
TPSA (A ²)	20.23	0	77.38	86.61	20.23	36.92	59.67
Rotatable Bonds	6	1	4	5	13	4	1
Lipinski violations	Yes, 1	Yes	Yes	Yes	Yes 1	Yes	Yes
Ghose	No, 3	Yes	Yes	Yes	No 1	Yes	Yes
Veber	Yes	Yes	Yes	Yes	No 1	Yes	Yes
Egan	No 1	Yes	Yes	Yes	No 1	Yes	Yes
Muegge	No 2	No 2	Yes	Yes	No 2	Yes	No 1

Table II: ADMET/Pharmacokinetics Properties of Selected Compounds

Properties	Parameters	L1	L2	L3	L4	L5	L6	L7
Absorption	Human intestinal absorption	HIA+						
	P-Glycoprotein substrate	Substrate	Non-Substrate	Substrate	Substrate	Non-Substrate	Non-Substrate	Substrate
	P-Glycoprotein inhibitor	Inhibitor	Non-Inhibitor	Inhibitor	Inhibitor	Non-Inhibitor	Inhibitor	Non-Inhibitor
	Subcellular localization	Lysosome	Lysosome	Mitochondria	Mitochondria	Lysosome	Mitochondria	Mitochondria
Distribution	Blood-brain barrier	BBB+	BBB+	BBB+	BBB-	BBB+	BBB+	BBB+
	Caco-2 permeability	Caco2+						
Metabolism	CYP450 2C9 Substrate	Non-Substrate						
	CYP450 2D6 Inhibitor	Non-Substrate						
	CYP450 3A4 Inhibitor	Substrate	Substrate	Non-Substrate	Substrate	Non-Substrate	Non-Substrate	Non-Substrate
	CYP450 1A2 Inhibitor	Non-Inhibitor	Non-Inhibitor	Inhibitor	Non-Inhibitor	Non-Inhibitor	Inhibitor	Inhibitor
	CYP450 2C9 Inhibitor	Non-Inhibitor	Non-Inhibitor	Inhibitor	Inhibitor	Non-Inhibitor	Non-Inhibitor	Non-Inhibitor
	CYP450 2D6 Inhibitor	Non-Inhibitor						
	CYP450 2C19 Inhibitor	Non-Inhibitor	Non-Inhibitor	Inhibitor	Inhibitor	Non-Inhibitor	Non-Inhibitor	Non-Inhibitor
	CYP450 3A4 Inhibitor	Non-Inhibitor	Non-Inhibitor	Inhibitor	Inhibitor	Non-Inhibitor	Inhibitor	Non-Inhibitor
CYP Inhibitory Promiscuity	low	low	High	High	low	High	low	
Excretion	Renal Organic Cation Transporter	Non-Inhibitor						
	Biodegradation	Not Ready						
Toxicity	AMES Toxicity	Non-Toxic						
	Carcinogens	Non-Carcinogens						
	Fish Toxicity	High						
	Tetrahymena Pyriformis Toxicity	High						
	Honey Bee Toxicity	High						
	Acute Oral Toxicity	I	III	III	III	III	III	III
	Carcinogenicity (Three-class)	Non required	Warning	Non required				
	Aqueous solubility	-4.7027	-3.633	-3.2979	-3.5650	-2.4720	-2.9883	-3.3060
	Caco-2 Permeability	1.5008	2.0486	1.0547	1.1739	1.2481	1.1257	0.9465



Table III: Active Sites of PLA2 (1BK9)

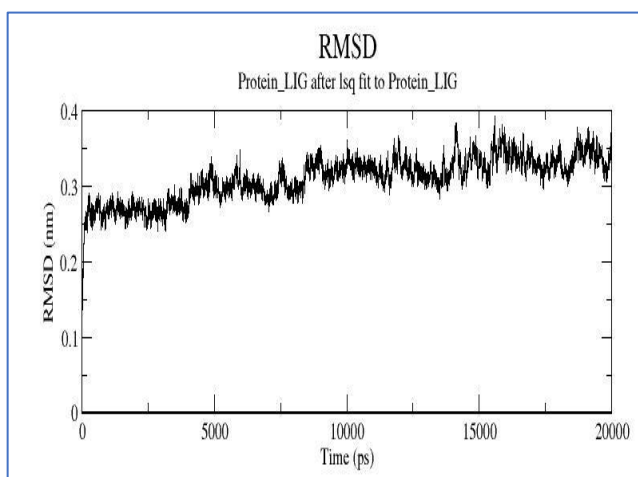
Molecule	1	1	1	1	1	1	1	1	1	1	1	1	1	1
Chain	A	A	A	A	A	A	A	A	A	A	A	A	A	A
Residue	31	2	106	52	5	29	9	31	43	18	45	48	49	99
Type	TRP	LEU	PHE	TYR	PHE	CYS	ILE	GLN	ARG	ALA	CYS	HIS	ASP	ASP

Table-IV: Docking Results of Ligand – Receptor Interaction

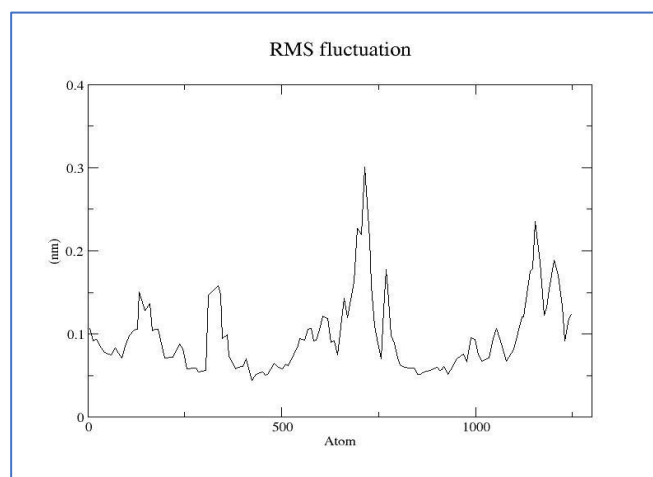
Compound name	ID	Docking score (Kcal/mol)	H- bonds(Å)	Bonding Residues
L1	222284	-10.54	-	LUE2, PHE5, GLU6, ILE9, GLY18, MET19, TYR22, TYR28, CYS29, GLY30, TRP31, GLY32, CYS45, HIS48, ASP49, TYR52
L2	5369483	-6.81	-	PHE5, ILE9, GLY18, TYR22, SER23, TYR28, CYS29, GLY30, CYS45, HIS48, ASP49, PHE106
L3	73399	-8.45	TYR22(2.80Å), GLY32(3.02 Å), HIS48(3.28 Å)	PHE5, TYR22, SER23, GLY30, TRP31, GLY32, CYS45, HIS48, ASP49, TYR52, LYS68, PRO68, PHE106
L4	181681	-7.09	ASP49(2.59 Å)	LUE2, LEU3, PHE5, GLU6, ILE9, GLY18, MET19, TYR22, SER23, GLY30, TRP31, CYS45, HIS48, ASP49, TYR52, PHE106
L5	5280435	-6.78	GLY32(2.66 Å), ASP49(3.07 Å)	LUE2, PHE5, GLU6, ILE9, GLY18, MET19, TYR22, SER23, GLY30, TRP31, GLY32, CYS45, HIS48, ASP49, TYR52, PHE106
L6	10231	-5.77	GLY30(3.08 Å), HIS48(3.22 Å)	LUE2, PHE5, ILE9, GLY18, TYR22, SER23, TYR28, CYS29, GLY30, CYS45, HIS48, ASP49, TYR52
L7	5280460	-5.82	CYS45 (3.29 Å), HIS48(2.98 Å), ASP49(2.53 Å)	PHE5, ILE9, GLY18, TYR22, GLY30, TRP31, GLY32, CYS45, HIS48, ASP49, PHE106

Table V: Ramachandran plot Analysis of 1BK9

Physicochemical Properties	1bk9	
	No of Residues	% Target
Most Favoured Regions [A, B, L]	96	91.4
Additional Allowed Regions [A,B,L,P]	9	8.6
Generously Allowed Regions [~A,~B,~L,~P]	0	0
Disallowed Regions [XX]	0	0
Non-Glycine And Non-Proline Residues	105	100
End-Residues (Excl. Gly And Pro)	3	
Glycine residues	12	
Proline residues	5	
Total number of residues	125	



[Fig.3: RMSD Graph of Phospholipase A2 (1BK9) -Beta Sitosterol Complex]



[Fig.4: RMSF Graph of Phospholipase A2 (1BK9) – Beta Sitosterol Complex]

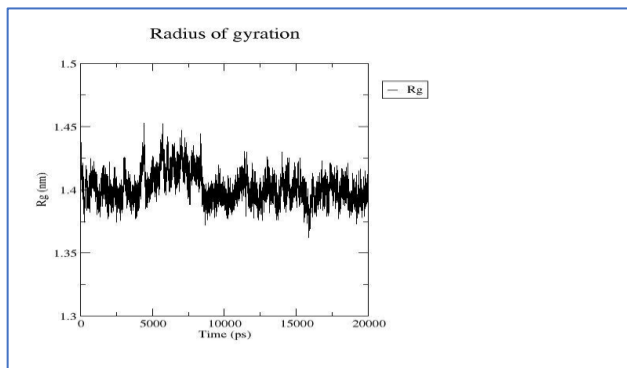


[Fig.5: GYRATION Graph of PhospholipaseA2 (1BK9) – Betasitosterol Complex]

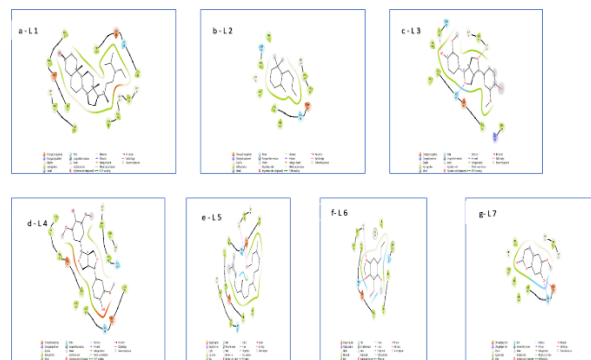


[Fig.8: 2D Representation of Ligand-Receptor Interaction]

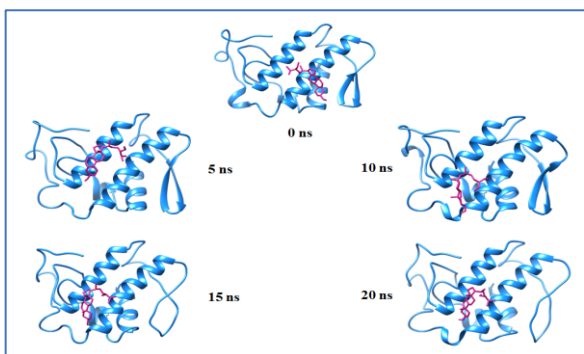


[Fig.6: Conformational Changes of the PLA2 (1BK9) – Beta Sitosterol Complex During Simulation]

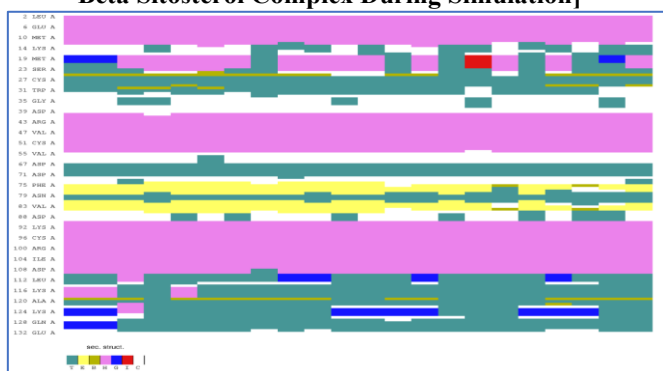


[Fig.7: Timeline of the PLA2 (1BK9) – Beta Sitosterol Complex During Simulation]

Disclaimer/Publisher’s Note: The statements, opinions and data contained in all publications are solely those of the individual author(s) and contributor(s) and not of the Lattice Science Publication (LSP)/ journal and/ or the editor(s). The Lattice Science Publication (LSP)/ journal and/or the editor(s) disclaim responsibility for any injury to people or property resulting from any ideas, methods, instructions, or products referred to in the content.